Use of glass waste in the production of metakaolin-based geopolymer submitted to room temperature and thermal curing

Utilização de resíduo de vidro na produção de geopolímero de base metacaulim submetido a cura ambiente e em estufa

Cristiane do Bom Conselho Sales Alvarenga
Rosemary do Bom Conselho Sales
Rodrigo Barreto Caldas
Paulo Roberto Cetlin
Maria Teresa Paulino Aguilar

Abstract

Metakaolin is the principal raw material utilized in the synthesis of geopolymers, although its ratio of silica and alumina contents is not ideal. Normally, the SiO_2 content is adjusted with the use of silicates present in the activating solution. An eco-efficient alternative would be the use of glass waste as an additional source of silica. This work evaluates the efficiency of the alkaline activation of metakaolin, using potassium hydroxide and silicate, with and without the substitution of 12.5% of metakaolin by microparticles of glass. The efficiency of the alkaline activation was evaluated by X ray diffractometry, spectroscopy in the infrared region with the Fourier transform, nuclear magnetic resonance spectroscopy of ^{27}Al and ^{29}Si, specific mass and compressive strength. The results indicate the occurrence of geopolymerization with and without the use of glass waste. It was observed that the substitution of 12.5% favors the mechanical performance of the compounds at 28 days, with increases by 37% and 47% in the mechanical strength of the material with thermal curing and ambient temperature curing, respectively.

Keywords: Metakaolin. Glass waste. Potassium hydroxide. Alkaline activation. Geopolymerization.

[1]Cristiane do Bom Conselho Sales Alvarenga
[1]Universidade Federal de Minas Gerais
Belo Horizonte – MG – Brasil

[2]Rosemary do Bom Conselho Sales
[2]Universidade do Estado de Minas Gerais
Belo Horizonte – MG – Brasil

[3]Rodrigo Barreto Caldas
[3]Universidade Federal de Minas Gerais
Belo Horizonte – MG – Brasil

[4]Paulo Roberto Cetlin
[4]Universidade Federal de Minas Gerais
Belo Horizonte – MG – Brasil

[5]Maria Teresa Paulino Aguilar
[5]Universidade Federal de Minas Gerais
Belo Horizonte – MG – Brasil

Recebido em 09/08/20
Aceito em 08/08/21

Resumo

O metacaulim é a principal matéria-prima utilizada na síntese de geopolímeros, embora a relação entre os teores de sílica e alumina não seja a ideal. Normalmente, o teor de SiO_2 é ajustado com o uso de silicatos presentes na solução ativadora. Uma opção ecoeficiente seria o uso de resíduos de vidro como fonte adicional de sílica. Este trabalho avalia a eficiência da ativação alcalina do metacaulim, utilizando hidróxido e silicato de potássio, com e sem substituição de 12,5% de metacaulim por micropartículas de vidro. A eficiência da ativação alcalina foi avaliada por difratometria de raios x, espectroscopia na região infravermelha com transformada de Fourier, espectroscopia de ressonância magnética nuclear do ^{27}Al e ^{29}Si, massa específica e resistência à compressão. Os resultados indicam a ocorrência de geopolimerização com e sem uso de resíduo de vidro. Observou-se que a substituição de 12,5% favorece o desempenho mecânico dos compósitos aos 28 dias, com aumentos de 37% e 47% da resistência mecânica do material com cura em estufa e na temperatura ambiente, respectivamente.

***Palavras-chave**: Metacaulim. Resíduo de vidro. Hidróxido de potássio. Ativação alcalina. Geopolimerização.*

Introduction

Geopolymers are an advantageous alternative to Portland cement in certain applications. Depending on the raw materials and the processing conditions, these materials can present high initial compressive strength, low shrinkage, greater/lower consistency, resistance to acid and sulfate attack, and better thermal stability at high temperatures (RIAHI *et al*., 2020; SINGH; MIDDENDORF, 2020; TORRES-CARRASCO; PUERTAS, 2017). In addition, these binders present long-term mechanical strength and durability greater than Portland cement (DAVIDOVITS, 2017; HÁJKOVÁ, 2018; YASERI *et al*., 2017).

Geopolymer binders can be obtained by the alkaline activation of aluminosilicate-rich raw materials (precursors) with low calcium content, such as calcined clays (especially metakaolin) and fly ashes, forming an amorphous or nanocrystalline sodium-aluminosilicate hydrates gel (N-A-S-H), with a tridimensional structure charge-balanced by cations from an alkali activator (BERNAL; PROVIS, 2014; PROVIS; LUKEY; VAN DEVENTER, 2005). Geopolymers can be synthesized following two routes (FENG; PROVIS; VAN DEVENTER, 2012). In the usual two-part method, the alkaline activator is typically a solution of sodium hydroxide, potassium hydroxide or sodium or potassium silicates in high concentrations (LAHOTI; TAN; YANG, 2019). In the one-part method, a dry mixture of an alkaline source powder and a precursor receive water addition (KOLOUŠEK *et al*., 2007).

Studies by Dimas, Giannopoulou and Panias (2009) indicate that it is necessary to add a silica source in most precursors to adjust the Si/Al ratio and consequently improve the performance of the materials produced. A proportion of Si: Al of 3:1 is considered adequate (YASERI *et al*., 2017). The presence of a fine and amorphous silica source could increase the formation of Si-O-Si bonds in the binder, which becomes more compact and with greater mechanical strength (GAO *et al*., 2014; HE *et al*., 2016).

Geopolymers can become eco-efficient binders for civil construction if sourced from local raw materials (ABDULKAREEM *et al*., 2021; ADESANYA *et al*., 2021; PROVIS, 2018). According to Singh, Kumar and Rai (2020), any residuals that contain aluminosilicates, when treated with alkaline solutions, can produce geopolymer cement. The incorporation of residues with an adequate Si/Al ratio could minimize the proportion of silicate solution used (HABERT; D'ESPINOSE DE LACAILLERIE; ROUSSEL, 2011; YASERI *et al*., 2017), besides promoting adequate disposal of an environmental liability (LIU *et al*., 2019; THO-IN *et al*., 2018). Studies by different authors analyze the use of glass as a precursor for obtaining geopolymers (CYR; IDIR; POINOT, 2012; PAVLIN *et al*., 2021) and indicate that a percentage of CaO and low Al content in the precursor waste glass promote the formation of calcium aluminosilicate, hydrate gel (C-A-S-H), together with N-A-S-H, influencing the mechanical properties of the activated material (THO-IN *et al*., 2018; TORRES-CARRASCO; PUERTAS, 2017; WALKLEY *et al*., 2016).

Regarding activators, sodium and potassium silicates and hydroxides are the most used (ADESANYA *et al*., 2021; DAVIDOVITS, 2017). The synthesis with sodium solutions having lower cost, wide availability, and low viscosity (PROVIS; BERNAL, 2014). The use of potassium activators favors zeolithization in geopolymer systems, but the crystallization rate is slower and rheology more favorable compared with their NaOH containing counterparts. The difference in ion size is likely to be a determining factor in reaction kinetics due to the tendency of the potassium cation to favor the formation of larger silicate oligomers (PROVIS; VAN DEVENTER, 2009).

Benavent, Frizon and Poulesquen (2016) compared geopolymers produced with sodium and potassium hydroxides in terms of the intrinsic porosity of the material and demonstrated that the use of the potassium activator leads to higher porosity and smaller pore sizes when the alkali silicate solution is prepared with the same silicate source. Different researchers studied the role of alkaline cations (Na^+ and K^+) in the geopolymerization reaction and observed that the compressive strength of Na^+ systems was higher than that of systems using K^+ with the same Si/Al ratio and alkali cation concentration (ABDUL RAHIM *et al*., 2015; ZHANG *et al*., 2017; SORE *et al*., 2020). However, results of Esparham, Moradikhou and Avanaki, (2020) showed that using NaOH provided greater 3- and 7- day compressive strengths and using KOH resulted in higher 28-day compressive strength. According to El Alouani *et al*. (2020) the fire resistance study revealed that the geopolymer binders induced by KOH are stable up to 600 °C. Hosan, Haque and Shaikh, (2016) show that the geopolymer synthesized with potassium-based activators is more stable at elevated temperatures than its sodium-based counterparts in terms of higher residual compressive strengths, lower mass loss, lower volumetric shrinkage and lower cracking damage. Results obtained by Novais *et al*. (2016) and Si *et al*. (2020) using metakaolin and glass waste activated with NaOH showed that the incorporation of about 11% of the glass waste increased the compressive strength, while larger amounts showed the opposite result compared with the metakaolin-based geopolymer.

It is observed that there are still inconclusive points about the use of activators. Thus, focusing on the geopolymerization reaction, this study evaluates the efficiency of alkaline activation of metakaolin using Potassium Hydroxide and Potassium Silicate solution with and without partial replacement of 12.5% of the precursor weight by microparticles of glass waste, using room temperature and thermal curing. These wastes come from the grinding of cut and drilling leftovers which are discarded in landfills, constituting an environmental liability. Thus, it is expected to contribute to the environment and knowledge, associating the use of glass waste with the KOH activator and cure at room temperature.

Materials and methods

Geopolymers were synthesized using the following precursors: commercial metakaolin with a high degree of purity; microparticles of amber soda-lime glass obtained from the breakage of larger particles and/or from cuttings from the glass industry. The chemical composition and physical properties of metakaolin and glass waste are shown in Table 1.

In metakaolin the molar ratio is 2.3. To obtain a polysialate-syloxo structure, a ratio of 3.3 to 4.5 would be required (KHALE; CHAUDHARY, 2007). Thus, it was necessary to use an alternative source of silica. In this study we opted for potassium silicate. Although rich in silica, glass waste has a SiO_2/Al_2O_3 molar ratio of 151.0, which indicates that its activation would not lead to the formation of aluminum tetrahedra, delaying curing time (CYR; IDIR; POINOT, 2012). For this reason, we chose to utilize it together with metakaolin.

The new precursor proposed in this research, consisting of 12.5% glass in place of metakaolin, would have a molar ratio of 2.7, therefore higher than that of metakaolin. This notwithstanding, it would still require the association of silicate with the activator. Glass waste incorporation into the precursor increases CaO content, which in metakaolin is 0.1%. The metakaolin particles have a medium size and specific surface larger than the glass waste ones, indicating greater surface roughness and, consequently, greater reactivity of these materials.

Potassium hydroxide and silicate were used for activation. High purity potassium hydroxide (86.1%) and deionized water were used to prepare the 10 mol KOH activator solution. Potassium Silicate solution (weight percentage: 12.8% K_2O, 27.4% SiO_2, and 59.8% H_2O) was also used as activator and as an additional source of silica.

The structure and phases present of precursors were evaluated by X-ray diffraction (XRD) and spectroscopy in the Infrared region with Fourier transform (FTIR) and nuclear magnetic resonance (NMR) of ^{29}Si and ^{27}Al. For XRD, a Rigaku Geigerflex D/max-Series diffractometer, with CuKα radiation, 10-80°, 0.02° 2θ step-scan, and 10 s/step were used. FTIR was performed on Bruker Tensor 27 equipment, with Golden gate ATR accessory, 4 cm^{-1} resolution, 256 scans, in the absorbency mode. Moreover, Bruker Ascend 700 MHz solid-state NMR equipment with 16.4 Tesla field allowed the observation of ^{27}Al at 139.09 MHz by single pulse analysis with magic-angle rotation in a 4 mm rotor system at 14.0 kHz, 0.5 s repetition time, and 0.28 μs pulse. The ^{29}Si observation tests were performed on Bruker 400 UltraShield equipment, with 9.4 Tesla field and 79.49 MHz frequency, using single pulse analysis with angle rotation in a 7 mm rotor system at 5 kHz, 60 s repetition time, and 2.11 μs pulse.

Table 1 - **Chemical composition and physical properties of metakaolin and glass waste**

Chemical composition (%)											
	SiO_2	Al_2O_3	CaO	K_2O	Fe_2O_3	TiO_2	MgO	Na_2O	SO_3	Other	LOI*
Metakaolin	51.3	38.0	0.1	2.8	2.6	1.6	0.9	0.1	0.04	2.6	2.2
Glass waste	72.9	0.8	9.2	0.02	0.7	-	3.6	6.0	0.3	6.6	0.4
				Metakaolin			**Glass waste**				
SiO_2/Al_2O_3 Molar Ratio				2.3			151.0		-	-	-
Average particle size d_{50} (μm)				11.8			7.6		-	-	-
Maximum particle size d_{90} (μm)				36,0			37.8		-	-	-
Gas adsorption BET (m^2/g)				14.5			3.0		-	-	-

Note: *loss of ignition.

Based on the results of Novais *et al*. (2016), the samples were prepared with 100% metakaolin (Geo-Ref.) and by replacing 12.5% of this weight by glass waste (Geo-Glass). Table 2 presents the proportions and molar ratios of the mixtures with and without glass waste (Geo-Ref and Geo-Glass, respectively), calculated based on the chemical composition of the precursor materials and activating solution. Increasing the SiO_2/Al_2O_3 molar ratio was also considered to promote positive effects on compressive strength; however, there is a threshold from which this strength decreases (NOVAIS *et al*., 2016). Thus, using potassium silicate in the preparation of geopolymers increased the molar ratio of the mixtures from 2.3 to 3.3 in reference geopolymers, and from 2.7 to 3.9 in glass waste geopolymers, both within the limits (3.3 to 4.5) recommended in the literature.

In determining activator content (Table 2), the following limits were used for the best performance of geopolymers: K_2O/Al_2O_3 (0.8-1.6); K_2O/SiO_2 (0.2-0.48); H_2O/K_2O (10.0-25.0) (KHALE; CHAUDHARY, 2007). Moreover, viscosity control included the analysis of the H_2O/K_2O molar ratio, since the presence of water is important for ion mobility during dissolution, but its excess reduces the alkalinity of the solution and decreases the reaction rate.

Potassium hydroxide and silicate were used in a combination. The preparation of geopolymer pastes first involved homogenizing the potassium silicate and KOH solution in a mechanical mixer for about 2 min., obtaining an alkaline activator solution. The activator solution was added to previously oven dried metakaolin and/or metakaolin/glass. After mechanical homogenization at room temperature for 7 min., the mixtures were subjected to mechanical vibration for 5 min. for removal of air bubbles.

The activated material was then poured into PVC (DEUTSCHES…, 2012) cylindrical molds previously greased with liquid Vaseline to facilitate demolding. The various PVC molds containing the geopolymer were placed inside a silicone mold for stability and were again vibrated for about 10 min. to remove air bubbles, formed during the preparation of the activators, and to ease mold filling. To ensure the flat and even geometry of the exposed surfaces, all specimens were placed between two plumb leveled glass plates and wrapped in plastic film. Part of the samples was cured at room temperature (Geo-Ref-RO and Geo-Glass-RO) and part thermally cured at 40 °C for 24 hours (Geo-Ref-TH and Geo-Glass-TH). The samples were then demolded and kept at room temperature, being wrapped in plastic for another 27 days.

The occurrence of geopolymerization was analyzed after 28 days of curing by XRD, FTIR, and NMR of the ^{29}Si and ^{27}Al at the same conditions used to characterize the precursors.

The specific mass and compressive strength of the synthesized pastes were also evaluated after 24h, 7 days, and 28 days of cure. Three specimens of each mixture were tested for each age. After demolding, specimens had their mass and dimensions measured with a precision scale (Bel Engineering, Piracicaba, Brazil) and an IP65 caliper (Mitutoyo, Aurora, IL, USA). Based on this information, specific masses were determined. In the compressive strength test, an Instron 5582 universal machine with a capacity of 100 kN was used. The compression rate used in the test was 0.01 mm/s and load application occurred until rupture.

Table 2 - **Mixture/activator composition and atomic/molar ratios**

	Identification	Geo-Ref-10 mol	Geo-Glass-10 mol
Molar ratios	SiO_2/Al_2O_3 (no silicate)	2.3	2.7
	SiO_2/Al_2O_3	3.3	3.9
	K_2O/Al_2O_3	1.0	1.1
	K_2O/SiO_2	0.3	0.3
	H_2O/K_2O	14.2	14.2
Mixture composition (%)	Metakaolin	41.2	36.0
	Glass waste	0.0	5.1
	K_2SiO_3	34.2	34.2
	KOH (10 mol/l)	24.7	24.7

Results and discussions

Characterization of precursors

Based on the diffractograms in Figure 1, metakaolin shows the presence of the following crystalline phases: kaolinite, quartz, muscovite, and anatase. The presence of a curved region (halo) formed by the deviation from the baseline at 2θ = 18° to 30° can be attributed to amorphous aluminosilicates (DUXSON et al., 2007a; PROVIS; VAN DEVENTER, 2009). The presence of kaolinite and other crystalline phases is an indication of incomplete calcination of kaolinite which negatively influences geopolymerization (BENEZET; BENHASSAINE, 2009; MENEZES *et al*., 2018). The diffuse spectrum observed throughout the glass waste diffractogram, as well as the halo present at 2θ = 15° to 35°, indicate that the material is amorphous (TORRES-CARRASCO, 2015). Considering that predominantly amorphous materials are more reactive than crystalline ones (SCRIVENER; NONAT, 2011), it can be inferred that the use of glass waste as a partial substitute for metakaolin would facilitate geopolymer synthesis.

The results obtained by Fourier transform infrared (FTIR) spectroscopy for metakaolin and glass waste are shown in Figure 2. The metakaolin spectrum shows vibrations at 1006 cm^{-1} that were related to Si-O-Al stretching vibrations. Lower values in the range from 1000 to 1100 cm^{-1} would correspond to greater incorporation of aluminum into the aluminosilicate structure. Moreover, Si-O-M (M: alkali metal) stretching vibrations near 910 cm^{-1} were also detected.

Figure 1 - **X-ray diffractogram of metakaolin and glass waste**

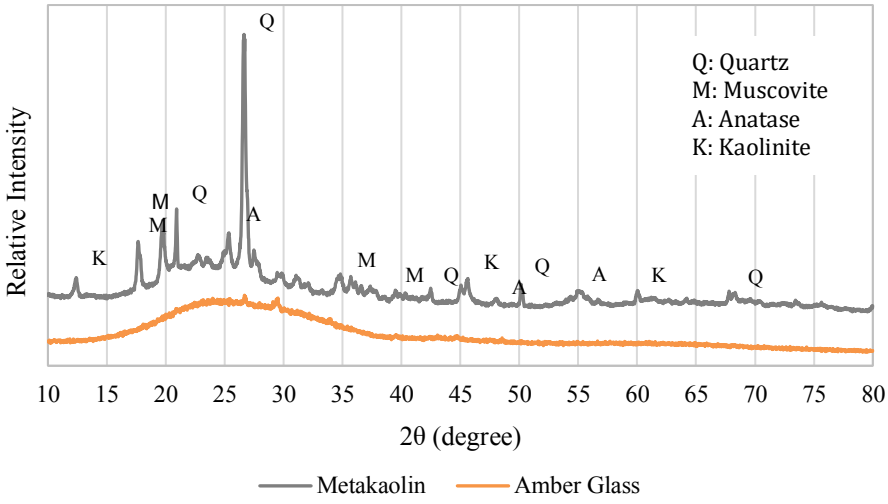

Figure 2 - **Infrared Spectroscopy results for metakaolin and glass waste**

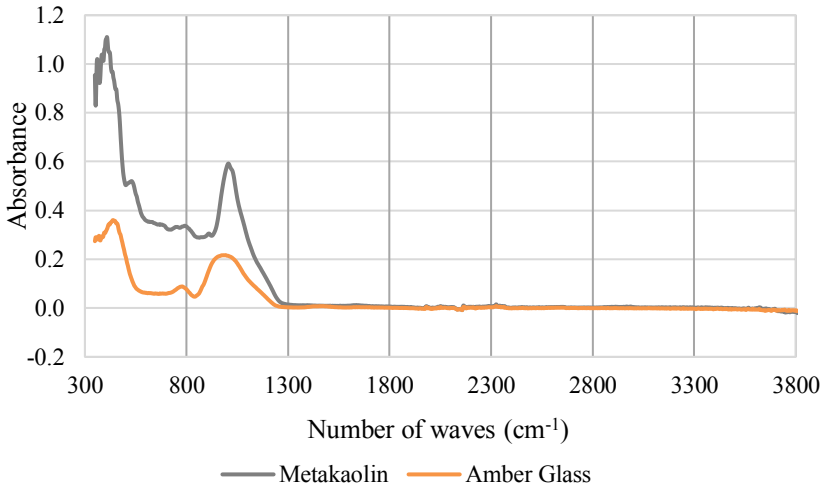

Four peaks of lower intensity were detected in the 791, 754, 678, and 529 cm^{-1} bands. Although not fully within the ranges described by Zhang *et al*. (2012), the following relationships can be inferred from Table 3: symmetric Si-O-Si stretching vibrations in quartz at 791 cm^{-1}; symmetric Al-O-Al stretching vibrations in tetrahedral coordination at 754 and 678 cm^{-1}; symmetric Al-O-Si stretching vibrations at 529 cm^{-1}. In the literature, the lowest vibrations cited are near 450 cm^{-1}, corresponding to the bending of Si-O-Si bonds, and could be related to the vibrations detected at 408 cm^{-1}. Between 1300 cm^{-1} and 3800 cm^{-1}, no significant disturbance is observed, indicating the absence of hydration water (3450 and 1650 cm^{-1}) in the precursor materials. Thus, the metakaolin spectrum indicates the existence of a continuous and random network of amorphous aluminosilicates favorable to geopolymerization. The glass waste result shows three peaks around 992, 778, and 438 cm^{-1}, which refer to the SiO_2 network. Similar results were found by Sales (2014). The 992 cm^{-1} band is probably related to asymmetric stretching of Si-O-Si bonds, typical of amorphous glass structures. Vibrations at 778 cm^{-1}, related to symmetric Si-O-Si stretching, and at 438 cm^{-1}, attributed to O-Si-O angular deformation, were detected. These results would confirm glass waste amorphousness.

The ^{27}Al spectrum obtained by nuclear magnetic resonance for metakaolin is shown in Figure 3. According to Duxson (2006), aluminum in the tetrahedral (AlO_4), pentahedral (AlO_5), and hexahedral (AlO_6) coordination are highly reactive and during geopolymerization reaction they are converted into tetrahedral sites associated with an alkali cation to maintain electron neutrality. The obtained spectrum showed the presence of signals at 55 ppm for tetrahedral coordination, at 30 ppm for pentahedral coordination, and at 5 ppm for hexahedral coordination. According to the same author, approximately equal proportions of aluminum are found in the mentioned coordination frameworks for metakaolin. In the present study, however, aluminum in hexahedral coordination is in greater proportion, indicating the presence of kaolinite, which could decrease the extent of geopolymerization (BENEZET; BENHASSAINE, 2009; MENEZES *et al*., 2018).

Table 3 – **Assignment of absorption bands obtained by infrared spectroscopy for metakaolin and glass waste**

cm^{-1}	Metakaolin	cm^{-1}	Glass Waste
1006	Si-O-Al (*stretching*)	992	Si-O-Si (*stretching*)
901	Si-O-M (stretching)	778	Si-O-Si (*stretching*)
791	Si-O-Si (*stretching*)	438	O-Si-O (*bending*)
754/768	Al-O-Al (*stretching*)		
529	Al-O-Si (*stretching*)		
408	Si-O-Si (*bending*)		

Figure 3 – **Nuclear magnetic resonance of metakaolin (^{27}Al solid-state)**

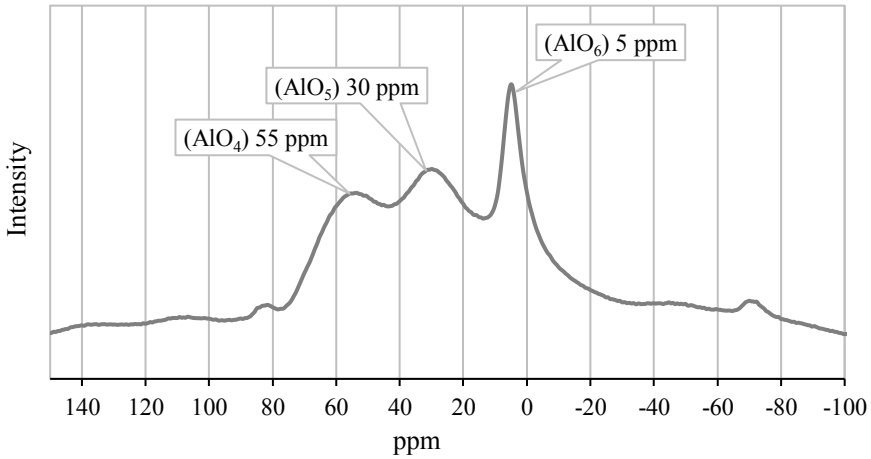

The ^{29}Si spectrum obtained by NMR for metakaolin is shown in Figure 4. According to Lecomte *et al.* (2003) and Duxson (2006) the signal near -92 ppm is attributed to kaolin silicates and represents a Si nucleus bonded to 3 other silicon atoms by covalent bonding (Q^3). After calcination, the same authors argue that crystallinity is expected to be lower, with the material showing a single peak at approximately -107 ppm, which can be attributed to a Si nucleus bonded to 4 other silicon atoms (Q^4). According to Valcke *et al.* (2015) this resonance would be close to -100 ppm. Rowles *et al.* (2007) describe a broad resonance for metakaolin at 104.8 ppm (Q^4 (1Al) - Q^4 (0Al)), which would be indicative of highly disordered structural networks. In this study, metakaolin showed signals around -107 ppm and -9 ppm, reinforcing the results of x-ray diffraction and infrared spectroscopy, which showed that the material was not properly calcined. The signal width indicates that this is an amorphous structure formed on kaolinite calcination.

Characterization of geopolymers

XRD and FTIR analysis

The XRD patterns of geopolymers after curing for 28 days are shown in Figure 5, along with that of metakaolin. The position of the diffraction peaks at 2θ = 26° in the geopolymers coincides with those of metakaolin, indicating the presence of quartz, i.e., unreacted material in the geopolymers. There is a halo in all geopolymer samples, corresponding to the existence of an amorphous phase, between 2θ = 20° to 35°, being displaced in relation to metakaolin (2θ = 18° to 30°). This change has been associated with the formation of new amorphous phases, being indicative of geopolymeric reaction (DUXSON *et al.*, 2007b; PROVIS; VAN DEVENTER, 2009). The position of the diffraction peak of geopolymer samples with and without glass waste coincides with the metakaolin peak. This occurs probably because of the low waste glass content used.

Figure 4 - **Nuclear magnetic resonance of metakaolin (^{29}Si solid-state)**

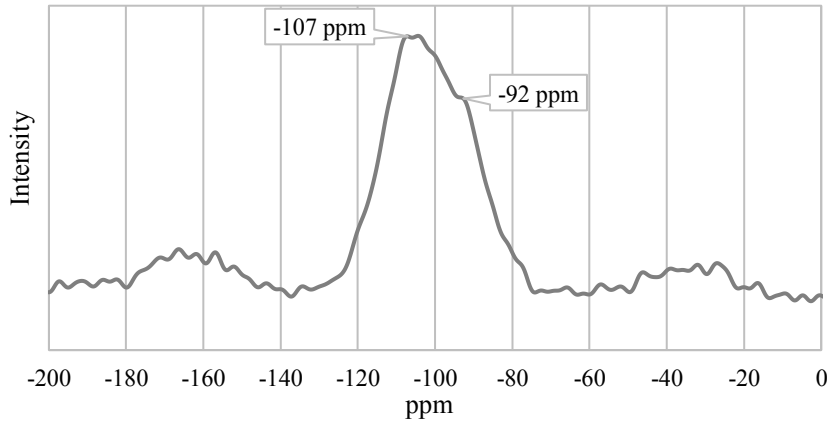

Figure 5 - **X-ray diffractogram of geopolymers**

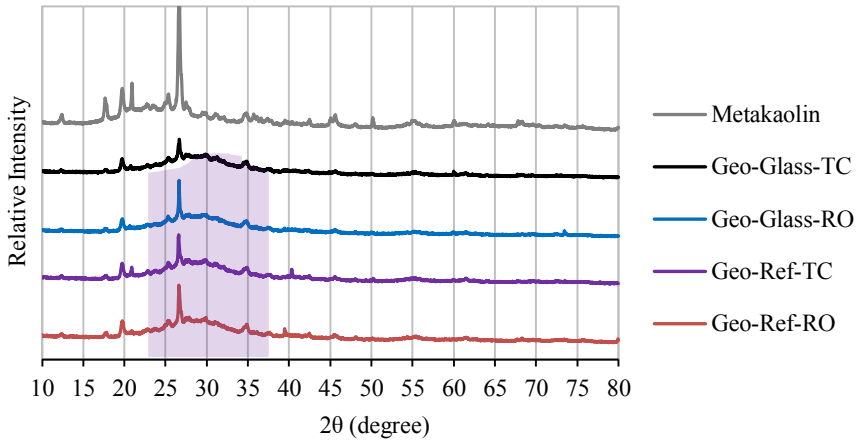

The spectra shown in Figure 6 were obtained by infrared spectroscopy for geopolymers cured for 28 days. There is no difference in the geopolymer spectra. However, there is a shift from the 1006 cm^{-1} band in metakaolin to 970 cm^{-1} in geopolymers. Valcke *et al*. (2015) describe that this shift to lower wavelengths in geopolymers occurs by the increased proportion of Al atoms in the tetrahedral position. This result indicates that geopolymerization reactions form a larger number of Si-O-Al bonds in the aluminosilicate structure. The bands around 3450 and 1650 cm^{-1} observed in the activated mixtures correspond to water resulting from geopolymerization.

Solid-state NMR analysis

The ^{27}Al spectra obtained by nuclear magnetic resonance of geopolymers and metakaolin are shown in Figure 7. Geopolymerization was notable in the geopolymer pastes produced, since a significant peak was observed in the range that characterizes tetrahedral coordination (55 ppm) and no pentahedral peaks (30 ppm) were identified. It is possible to identify peaks at approximately 5 ppm that would correspond to aluminum in hexahedral coordination, indicating the presence of uncalcined kaolinite, also identified in X-ray diffraction. This spectrum is similar to that observed in the studies by Duxson (2006) and Rowles *et al*. (2007), which associate it to geopolymerization and zeolite systems. No differences were observed regarding the presence of glass waste and curing type, indicating the contribution of waste to geopolymerization.

The ^{29}Si spectra obtained by nuclear magnetic resonance of geopolymers and metakaolin are shown in Figure 7. The signal near -92 ppm is shown to be permanent in all geopolymers, which may be related to kaolin silicates (LECOMTE *et al*., 2003). However, widening of this signal indicates the formation of a new, probably amorphous Q^3 structure. The strong signal reduction at -107 ppm would indicate that Q^4 units were consumed in the geopolymeric reaction (DUXSON, 2006). The peak intensity of thermally-cured samples is attenuated compared to room temperature cured samples, and the presence of glass waste does not interfere with the spectrum.

Apparent specific mass

The influence of curing type and glass waste incorporation on the apparent specific mass of geopolymers can be seen in Figure 8, where the average values as well as the amplitude of the measurements are presented. In all samples, the apparent specific mass decreased during curing, which can be attributed to the release of water that occurs during geopolymerization (NOVAIS *et al*., 2016; PIMRAKSA *et al*., 2011). The glass waste geopolymer cured at room temperature showed higher density at all three ages and, therefore, lower porosity. Considering that glass waste and metakaolin have close specific masses (2.5 and 2.6 g/cm^3, respectively), it was expected that the reference geopolymer had the largest specific mass due to its higher surface roughness. This would make it more reactive and, consequently, provide it with a denser and more resistant structure (NAZARI; BAGHERI; RIAHI, 2011). This fact did not occur probably due to the higher CaO content present in the glass waste sample. According to Khale and Chaudhary (2007), the formation of an amorphous and/or semicrystalline Ca-Al-Si structure reduces geopolymer porosity. The density of thermally-cured geopolymers is lower than that of those exposed to room temperature in the three analyzed ages (24 h, 7 days, and 28 days). The temperature of 40 °C may have induced an increase in the geopolymerization reaction rate, which consequently contributed to the increase of the water release rate. The thermally-cured glass waste sample had a higher density than the heat-treated reference, a trend similar to that observed at room temperature curing, probably due to the influence of calcium on the structure. The apparent specific mass obtained after 24h of thermal curing for the KOH-activated thermal sample is about the same as that obtained by Novais *et al*. (2016) in similar material activated with NaOH. At 28 days, however, the apparent specific mass of the KOH-activated glass waste thermal sample is superior.

Compressive strength

The influence of curing type and glass waste incorporation on compressive strength can be seen in Figure 9, where the average values and the amplitude of the measurements are presented. For all situations; compressive strengths above 26 MPa are obtained within 24 h.

Glass waste incorporation: the incorporation of 12.5% glass waste increased mechanical strength at 28 days from 25 MPa to 36 MPa for room temperature curing and from 27 MPa to 37 MPa for thermal curing. The replacement of metakaolin by glass waste increased the initial SiO_2/Al_2O_3 ratio with positive effects on strength. This occurs because Si-O-Si bonds are stronger than Si-O-Al and Al-O-Al bonds in geopolymers (BOBIRICĂ *et al*., 2015). Ozer and Soyer (2015) observed that compressive strength systematically

increased with increasing Si/Al molar ratio. Furthermore, using 10 mol NaOH, metakaolin, and fluorescent lamp glass waste, Novais *et al*. (2016) also observed an increase in compressive strength from 11.5 MPa to 15.5 MPa. In turn, Hao *et al*. (2013) reported that, after 28 days of curing, samples containing 10% of solar panel waste glass had compressive strengths of 12.5, 39.0, 63.3, and 66.7 MPa with solid-liquid ratio of 0.4, 0.6, 0.8, and 1.0, respectively.

Figure 6 - **Results of the Infrared Spectroscopy of geopolymers**

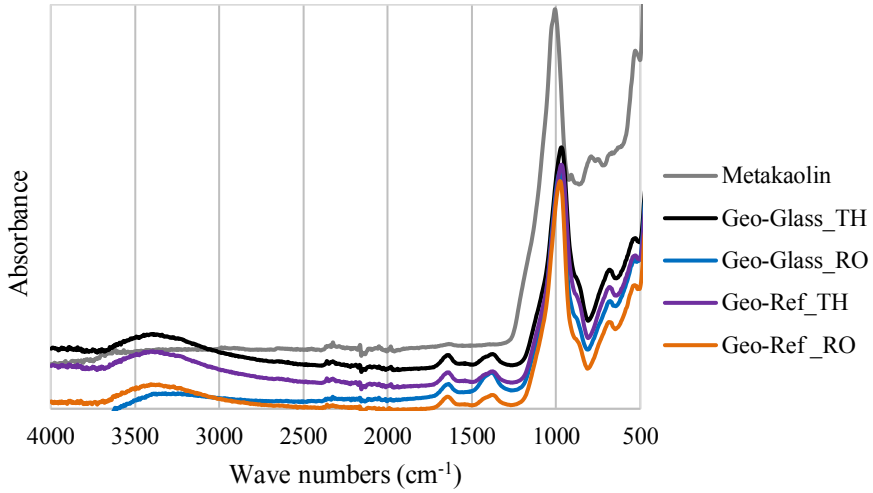

Figure 7 - **Nuclear magnetic resonance of geopolymers**

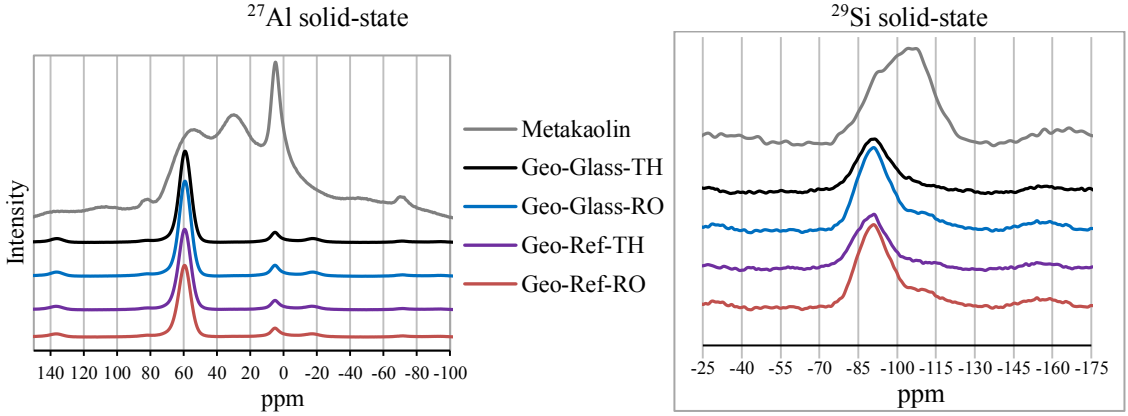

Figure 8 - **Apparent specific mass of geopolymers at 24h, 7 days, and 28 days**

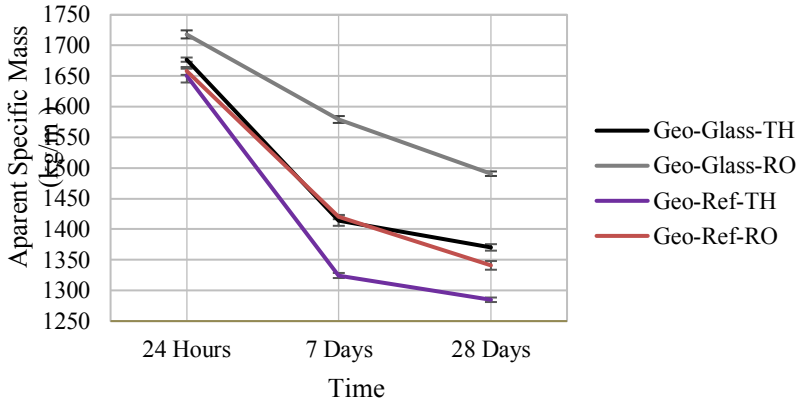

Figure 9 – **Compressive strength of geopolymers at 24h, 7 days, and 28 days**

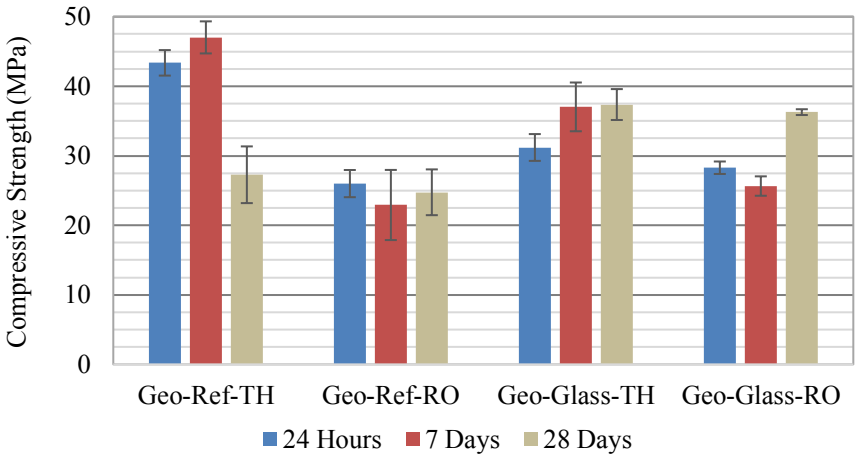

Thermally-cured glass waste-added samples achieved compressive strengths of 31 MPa in the first 24 hours, with a slight elevation at 7 days (37 MPa, remaining until 28 days). Glass waste incorporation increased the presence of CaO in the geopolymer matrix, which favored the formation of an amorphous and/or semicrystalline Ca-Al-Si structure, reducing porosity and increasing mechanical resistance (GARCIA-LODEIRO *et al*., 2011; KHALE; CHAUDHARY, 2007; XU *et al*., 2014). Room temperature cured glass waste-added samples reached compressive strengths of 28 MPa in the first 24hs, with a slight decrease at 7 days (26 MPa, which increased to 36 MPa at 28 days).

When cured at room temperature, glass waste does not appear to affect strength at an early age. Substitution with glass waste possibly reduced the release rates of silicon and aluminum ions due to the lower rate of glass waste dissolution compared to metakaolin, which would affect strength development (HAO *et al*., 2013).

Influence of curing type: for reference geopolymers wrapped in plastic film, without glass waste addition, curing at 40 ºC for 24 hours favored strength development in the early ages (43 MPa/24 hours; 47 MPa/7 days). However, at 28 days, this decreased significantly to 27 MPa. In the case of NaOH activator, the literature associates this decrease in compressive strength at 28 days with precipitation of silicates and aluminates due to excess Na^+ ions in the mixture. These destroy Si-O-Si stronger bonds, where one silicon atom is bonded to four other silicon atoms by covalent bonds (Q^4), forming Si-O-Na species, which are characterized as NBO (Nonbridging Oxygens) and show Q^2 (Si nucleus bonded to two other atoms) NMR coupling (ONORATO *et al*., 1985; ZIRL; GAROFALINI, 1992). Another possible explanation for this reduction in mechanical strength would be the formation of fissures caused by shrinkage (GUO; YANG, 2020; SI *et al*., 2020). However, in the case of thermal curing, glass waste-added geopolymers showed no decrease in strength at 28 days.

In the reference samples cured at room temperature, strength reached 26 MPa in 24 hours, decreasing to 23 MPa at 7 days, and with a slight increase at 28 days (25 MPa). Samples at 40 °C reached higher resistance at 24 hours and at 7 days compared to the samples cured at room temperature, an indication that the temperature increase in thermal curing accelerated the geopolymerization reaction. Nevertheless, reference samples cured thermally and at room temperature reached practically the same compressive strengths at 28 days (27 and 25 MPa, respectively). In some situations, compressive strength increases with age while their density diminishes. This could be related to the formation of expansive products with high compressive strength.

Conclusions

This study evaluates the use of microparticles of glass waste in the replacement of 12.5% metakaolin weight for the production of KOH/ Potassium silicate-activated geopolymers under room temperature and thermal curing. Replacing 12.5% metakaolin weight with glass waste increased the compressive strength at 28 days for both curing types. Glass waste replacement increased the initial reactive SiO_2/Al_2O_3 ratio with positive effects on compression strength, canceling a possible negative effect of the smaller specific surface of the glass on the reactivity of the precursors. It was also observed that glass waste incorporation increased the

density of room temperature cured samples. Furthermore, the presence of CaO probably contributed to the reduction of the geopolymer pores. This increase in density was not observed in thermal curing, possibly due to the high initial water release rate that would impair the calcium reaction in the structure. For metakaolin-based geopolymers, the curing type significantly affected strength development at early ages; however, at 28 days no significant differences were observed. Glass waste incorporation in thermal curing was beneficial for compressive strength at early ages; however, at 28 days the strengths in both curing types were similar. For samples of geopolymers with and without replacement of metakaolin with glass waste, 10mol KOH activation promoted compressive strengths above 26 MPa at 24 h, higher than the values found in the literature for 10mol NaOH. This research shows that it is possible to reintroduce an environmental liability in the production process of geopolymer which has compressive strength compatible with Portland cement pastes for use in structural concretes.

References

ABDUL RAHIM, R. H. *et al*. Comparison of using NaOH and KOH activated fly ash-based geopolymer on the mechanical properties. **Materials Science Forum**, v. 803, p. 179–184, sep. 2015.

ABDULKAREEM, M. *et al*. Environmental and economic perspective of waste-derived activators on alkali-activated mortars. **Journal of Cleaner Production**, v. 280, part 1, 2021.

ADESANYA, E. *et al*. Opportunities to improve sustainability of alkali-activated materials: a review of side-stream based activators. **Journal of Cleaner Production**, v. 286, 2021.

BENAVENT, V.; FRIZON, F.; POULESQUEN, A. Effect of composition and aging on the porous structure of metakaolin-based geopolymers. **Journal of Applied Crystallography**, v. 49, n. 6, p. 2116–2128, 2016.

BENEZET, J. C.; BENHASSAINE, A. Contribution of different granulometric populations to powder reactivity. **Particuology**, v. 7, n. 1, p. 39–44, 2009.

BERNAL, S. A.; PROVIS, J. L. Durability of alkali-activated materials: progress and perspectives. **Journal of the American Ceramic Society**, v. 97, n. 4, p. 997–1008, 2014.

BOBIRICĂ, C. *et al*. Influence of waste glass on the microstructure and strength of inorganic polymers. **Ceramics International**, v. 41, n. 10, p. 13638–13649, 2015.

CYR, M.; IDIR, R.; POINOT, T. Properties of inorganic polymer (geopolymer) mortars made of glass cullet. **Journal of Materials Science**, v. 47, n. 6, p. 2782–2797, 2012.

DAVIDOVITS, J. Geopolymers: ceramic-like inorganic polymers. **Journal of Ceramic Science and Technology**, v. 8, n. 3, p. 335–350, 2017.

DIMAS, D.; GIANNOPOULOU, I.; PANIAS, D. Polymerization in sodium silicate solutions: a fundamental process in geopolymerization technology. **Journal of Materials Science**, v. 44, n. 14, p. 3719–3730, 2009.

DEUTSCHES INSTITUT FÜR NORMUNG. **EN 12390-1**: european standards: testing hardened concrete: part 1: shape, dimensions and other requirements for specimens and moulds. Berlin, 2012.

DUXSON, P. **The structure and thermal evolution of metakaolin geopolymers**. Melbourne, 2006. Thesis - Faculty of Engineering, University of Melbourne, Melbourne, 2006.

DUXSON, P. *et al*. Geopolymer technology: the current state of the art. **Journal of Materials Science**, v. 42, n. 9, p. 2917–2933, 2007a.

DUXSON, P. *et al*. The role of inorganic polymer technology in the development of “green concrete”. **Cement and Concrete Research**, v. 37, n. 12, p. 1590–1597, 2007b.

EL ALOUANI, M. *et al*. Influence of the nature and rate of alkaline activator on the physicochemical properties of fly ash-based geopolymers. **Advances in Civil Engineering**, v. 2020, art. 8880906, p. 1-13, 2020.

ESPARHAM; MORADIKHOU, A. B.; AVANAKI, M. J. Effect of various alkaline activator solutions on compressive strength of fly ash-based geopolymer concrete. **Journal of Civil Engineering and Materials Application**, v. 4, p. 115–123, apr. 2020.

FENG, D.; PROVIS, J. L.; VAN DEVENTER, J. S. J. Thermal activation of albite for the synthesis of one-part mix geopolymers. **Journal of the American Ceramic Society**, v. 95, n. 2, p. 565–572, 2012.

GAO, K. *et al*. Effects SiO2/Na2O molar ratio on mechanical properties and the microstructure of nano-SiO2 metakaolin-based geopolymers. **Construction and Building Materials**, v. 53, p. 503–510, 2014.

GARCIA-LODEIRO, I. *et al*. Compatibility studies between N-A-S-H and C-A-S-H gels: study in the ternary diagram Na2O-CaO-Al2O3-SiO 2-H2O. **Cement and Concrete Research**, v. 41, n. 9, p. 923–931, 2011.

GUO, X.; YANG, J. Intrinsic properties and micro-crack characteristics of ultra-high toughness fly ash/steel slag based geopolymer. **Construction and Building Materials**, v. 230, 2020.

HABERT, G.; D'ESPINOSE DE LACAILLERIE, J. B.; ROUSSEL, N. An environmental evaluation of geopolymer based concrete production: Reviewing current research trends. **Journal of Cleaner Production**, v. 19, n. 11, p. 1229–1238, 2011.

HÁJKOVÁ, P. Kaolinite claystone-based geopolymer materials: effect of chemical composition and curing conditions. **Minerals**, v. 8, n. 10, p. 17–19, 2018.

HAO, H. *et al*. Utilization of solar panel waste glass for metakaolinite-based geopolymer synthesis. **Environmental Progress & Sustainable Energy**, v. 32, p. 797–803, 2013.

HE, P. *et al*. Effects of Si/Al ratio on the structure and properties of metakaolin based geopolymer. **Ceramics International**, v. 42, n. 13, p. 14416–14422, 2016.

HOSAN, A.; HAQUE, S.; SHAIKH, F. Compressive behaviour of sodium and potassium activators synthetized fly ash geopolymer at elevated temperatures: a comparative study. **Journal of Building Engineering**, v. 8, p. 123–130, 2016.

KHALE, D.; CHAUDHARY, R. Mechanism of geopolymerization and factors influencing its development: A review. **Journal of Materials Science**, v. 42, n. 3, p. 729–746, 2007.

KOLOUŠEK, D. *et al*. Preparation, structure and hydrothermal stability of alternative (sodium silicate-free) geopolymers. **Journal of Materials Science**, v. 42, p. 9267-9275, 2007.

LAHOTI, M.; TAN, K. H.; YANG, E. H. A critical review of geopolymer properties for structural fire-resistance applications. **Construction and Building Materials**, v. 221, p. 514–526, 2019.

LECOMTE, I. *et al*. Synthesis and characterization of new inorganic polymeric composites based on kaolin or white clay and on ground-granulated blast furnace slag. **Journal of Materials Research**, v. 18, n. 11, p. 2571–2579, 2003.

LIU, Y. *et al*. An overview on the reuse of waste glasses in alkali-activated materials. **Resources, Conservation and Recycling**, v. 144, p. 297–309, feb. 2019.

MENEZES, R. M. R. O. *et al*. Hydraulic binder obtained from recycled cement and sand powder. **Revista IBRACON de Estruturas e Materiais**, v. 11, n. 6, p. 1178–1185, 2018.

NAZARI, A.; BAGHERI, A.; RIAHI, S. Properties of geopolymer with seeded fly ash and rice husk bark ash. **Materials Science and Engineering A**, v. 528, n. 24, p. 7395–7401, 2011.

NOVAIS, R. M. *et al*. Waste glass from end-of-life fluorescent lamps as raw material in geopolymers. **Waste Management**, v. 52, p. 245–255, 2016.

ONORATO, P. I. K. *et al*. Bridging and nonbridging oxygen atoms in alkali aluminosilicate glasses. **Journal of the American Ceramic Society**, v. 68, n. 6, p. C148-C150, 1985.

OZER, I.; SOYER-UZUN, S. Relations between the structural characteristics and compressive strength in metakaolin based geopolymers with different molar Si/Al ratios. **Ceramics International**, v. 41, n. 8, p. 10192–10198, 2015.

PAVLIN, M. *et al*. Mechanical, microstructural and mineralogical evaluation of alkali-activated waste glass and stone wool. **Ceramics International**, fev. 2021.

PIMRAKSA, K. *et al*. Lightweight geopolymer made of highly porous siliceous materials with various Na_2O/Al_2O_3 and SiO_2/Al_2O_3 ratios. **Materials Science and Engineering A**, v. 528, n. 21, p. 6616–6623, 2011.

PROVIS, J. L. Alkali-activated materials. **Cement and Concrete Research**, v. 114, p. 40–48, 2018.

PROVIS, J. L.; BERNAL, S. A. Geopolymers and related alkali-activated materials. **Annual Review of Materials Research**, v. 44, n. 1, p. 299–327, 2014.

PROVIS, J. L.; LUKEY, G. C.; VAN DEVENTER, J. S. J. Do geopolymers actually contain nanocrystalline zeolites? a reexamination of existing results. **Chemistry of Materials**, v. 17, n. 12, p. 3075–3085, 2005.

PROVIS, J. L.; VAN DEVENTER, J. S. J. **Geopolymers, Structures, Processing, Properties and Industrial Applications**. Washington, DC: Woodhead Publishing; CRC Press LLC, 2009.

RIAHI, S. *et al*. The effect of mixing molar ratios and sand particles on microstructure and mechanical properties of metakaolin-based geopolymers. **Materials Chemistry and Physics**, v. 240, 2020.

ROWLES, M. R. *et al*. ^{29}Si, ^{27}Al, ^{1}H and ^{23}Na MAS NMR study of the bonding character in aluminosilicate inorganic polymers. **Applied Magnetic Resonance**, v. 32, p. 663–689, 2007.

SALES, F. A. **Estudo da atividade pozolânica de micropartículas de vidro soda-cal, incolor e âmbar, e sua influência no desempenho de compostos de cimento portland**. Belo Horizonte: Universidade Federal de Minas Gerais, 2014.

SCRIVENER, K. L.; NONAT, A. Hydration of cementitious materials, present and future. **Cement and Concrete Research**, v. 41, n. 7, p. 651–665, 2011.

SI, R. *et al*. Mechanical property, nanopore structure and drying shrinkage of metakaolin-based geopolymer with waste glass powder. **Journal of Cleaner Production**, v. 242, 2020.

SINGH, N. B.; KUMAR, M.; RAI, S. Geopolymer cement and concrete: Properties. **Materials Today: Proceedings**, v. 29, p. 743–748, 2020.

SINGH, N. B.; MIDDENDORF, B. Geopolymers as an alternative to Portland cement: an overview. **Construction and Building Materials**, v. 237, 2020.

SORE, S. O. *et al*. Comparative study on geopolymer binders based on two alkaline solutions (NaOH and KOH). **Journal of Minerals and Materials Characterization and Engineering**, v. 8, n. 6, p. 407–420, 2020.

THO-IN, T. *et al*. Compressive strength and microstructure analysis of geopolymer paste using waste glass powder and fly ash. **Journal of Cleaner Production**, v. 172, p. 2892–2898, 2018.

TORRES-CARRASCO, M. **Reutilización de residuos vítreos urbanos e industriales en la fabricación de cementos alcalinos. Activación, comportamiento y durabilidad**. Madrid: Universidad Autónoma de Madrid, 2015.

TORRES-CARRASCO, M.; PUERTAS, F. Waste glass as a precursor in alkaline activation: chemical process and hydration products. **Construction and Building Materials**, v. 139, p. 342–354, 2017.

VALCKE, S. L. A. *et al*. FT-IR and 29Si-NMR for evaluating aluminium–silicate precursors for geopolymers. **Materials and Structures**, v. 48, n. 3, p. 557–569, 2015.

WALKLEY, B. *et al*. Phase evolution of C-(N)-A-S-H/N-A-S-H gel blends investigated via alkali-activation of synthetic calcium aluminosilicate precursors. **Cement and Concrete Research**, v. 89, p. 120–135, 2016.

XU, H. *et al*. Effect of blast furnace slag grades on fly ash based geopolymer waste forms. **Fuel**, v. 133, p. 332–340, 2014.

YASERI, S. *et al*. The role of synthesis parameters on the workability, setting and strength properties of binary binder based geopolymer paste. **Construction and Building Materials**, v. 157, p. 534–545, 2017.

ZHANG, M. *et al*. A multiscale investigation of reaction kinetics, phase formation, and mechanical properties of metakaolin geopolymers. **Cement and Concrete Composites**, v. 78, p. 21–32, 2017.

ZHANG, Z. *et al*. Quantitative kinetic and structural analysis of geopolymers. Part 1. the activation of metakaolin with sodium hydroxide. **Thermochimica Acta**, v. 539, p. 23–33, 2012.

ZIRL, D. M.; GAROFALINI, S. H. Structure of sodium ahminosilicate glass surfaces David. **Journal of the Americun Ceramic Society**, v. 62, p. 2353–2362, 1992.

Cristiane do Bom Conselho Sales Alvarenga
Departamento de Engenharia de Estruturas | Universidade Federal de Minas Gerais | Av. Antônio Carlos, 6627, Bloco 2, Sala 4108, Pampulha | Belo Horizonte – MG – Brasil | CEP 31270-901 | Tel.: (31) 3409-3589 | E-mail: crisbcs@ufmg.br

Rosemary do Bom Conselho Sales
Departamento de Projeto e Configuração | Universidade do Estado de Minas Gerais | Rua Gonçalves Dias, 1434, Lourdes | Belo Horizonte – MG – Brasil | CEP 30140-091 | Tel.: (31) 98498-8077 | E-mail: rosemary.sales@uemg.br

Rodrigo Barreto Caldas
Departamento de Engenharia de Estruturas | Universidade Federal de Minas Gerais | E-mail: caldas@dees.ufmg.br

Paulo Roberto Cetlin
Departamento de Engenharia Mecânica | Universidade Federal de Minas Gerais | Av. Antônio Carlos, 6627, Bloco 2, Sala 3628, Pampulha | Belo Horizonte – MG – Brasil | CEP CEP 31270-901 | Tel.: (31) 3409-4891 | E-mail: pcetlin@demec.ufmg.br

Maria Teresa Paulino Aguilar
Departamento de Engenharia de Materiais e Construção | Universidade Federal de Minas Gerais | Av. Antônio Carlos, 6627, Bloco 2, Sala 3307, Pampulha | Belo Horizonte – MG – Brasil | CEP 31270-901 | Tel.: (31) 3409-1852 | E-mail: teresa@ufmg.br

Ambiente Construído
Revista da Associação Nacional de Tecnologia do Ambiente Construído
Av. Osvaldo Aranha, 99 - 3º andar, Centro
Porto Alegre – RS - Brasil
CEP 90035-190
Telefone: +55 (51) 3308-4084
www.seer.ufrgs.br/ambienteconstruido
www.scielo.br/ac
E-mail: ambienteconstruido@ufrgs.br